

PCCP

Accepted Manuscript



This is an *Accepted Manuscript*, which has been through the Royal Society of Chemistry peer review process and has been accepted for publication.

Accepted Manuscripts are published online shortly after acceptance, before technical editing, formatting and proof reading. Using this free service, authors can make their results available to the community, in citable form, before we publish the edited article. We will replace this *Accepted Manuscript* with the edited and formatted *Advance Article* as soon as it is available.

You can find more information about *Accepted Manuscripts* in the [Information for Authors](#).

Please note that technical editing may introduce minor changes to the text and/or graphics, which may alter content. The journal's standard [Terms & Conditions](#) and the [Ethical guidelines](#) still apply. In no event shall the Royal Society of Chemistry be held responsible for any errors or omissions in this *Accepted Manuscript* or any consequences arising from the use of any information it contains.

Fluorescence-detected Circular Dichroism Spectroscopy of Jet-cooled Ephedrine

Aram Hong,^a Changseop Jeong,^a Heeseon Jang,^a Myoung Choul Choi,^b Jiyoung Heo,^{*c}
and Nam Joon Kim^{*a}

^a*Department of Chemistry, Chungbuk National University, Chungbuk 361-763, Korea.*

^b*Mass Spectrometry & Advanced Instrument Group, Korea Basic Science Institute, Ochang
Center, Chungbuk 28119, Korea*

^c*Department of Biomedical Technology, Sangmyung University, Chungnam 330-720, Korea*

* Corresponding authors.

E-mail: jiyoungheo@smu.ac.kr (J. Heo), namjkim@chungbuk.ac.kr (N.J. Kim)

Abstract

The resonant two-photon ionization circular dichroism (R2PICD) spectrum represents the cumulative circular dichroism (CD) of one-photon excitation and the subsequent one-photon ionization, whereas the fluorescence-detected circular dichroism (FDCD) spectra exhibit only the CD of one-photon excitation, similar to conventional CD spectra. We obtained the FDCD spectra of jet-cooled ephedrine (EPD) near the origin band of the S_0 - S_1 transition to measure the CD of one-photon absorption and thus the CD of the ionization process in R2PI in comparison with the R2PICD spectra. The CD effects of the ionization following excitation of the A (0-0) and C (930 cm^{-1}) bands in the spectrum are small, whereas those of the B band are anomalously large, leading to opposite CD signs for the FDCD and R2PICD spectra. Based on the intermediate state-selective fragmentation patterns in the R2PI spectra, this large CD effect is attributed to the state-selective isomerization that occurs after excitation of the B band. Comparing the experimental and theoretical spectra, we determined that the B band corresponds to an asymmetric ring distortion mode that involves torsional motions of the side chain, which may facilitate the isomerization process. This study demonstrates that FDCD spectroscopy combined with R2PICD spectroscopy provides a powerful tool to measure the CD effects of the excitation and ionization processes separately in R2PI and thus probe the structural changes that occur during the ionization process following excitation to an intermediate state.

1 Introduction

Differential absorption of left- and right-handed circularly polarized (LCP and RCP, respectively) light by chiral compounds is called circular dichroism (CD). CD was first discovered in crystals by Hiding in 1847 and in chromium tartrate solutions by Cotton in 1895¹. With the advent of CD instrumentation in the early 1960s, CD spectroscopy has become a powerful tool to investigate the structures of and structural changes in chiral molecules in various chemical and biological reactions²⁻⁵.

Most CD spectroscopic studies have been performed in solution, where chiral compounds generally exist in many different conformations. Because CD is very sensitive to the structure of each conformer, the CD spectrum measured in solution shows only the average CD values, including the relative populations of all different conformers⁶. With this average CD spectrum, it is nearly impossible to acquire information regarding the structures of individual molecules. Thus, CD spectroscopy must be applied to molecules in an isolated gas phase, where different conformers can be distinguished spectroscopically⁷. However, the application of CD spectroscopy to gaseous molecules has been limited because of weak CD effects aggravated by a low number density of molecules and broad spectral features that arise from the high temperature of the gas cells in conventional CD spectrometers⁸⁻¹¹.

Compton and coworkers¹² first measured the CD of ion yields of 3-methylcyclopentanone (3-MCP) cooled by supersonic expansion using the resonance-enhanced multiphoton ionization (REMPI) technique. The CD of ion yields obtained using REMPI was also investigated using femtosecond laser pulses¹³. Boesl and coworkers¹⁴⁻¹⁷ determined the CD values of various organic molecules in a molecular beam using twin-peak mass spectrometry. Photoelectron CD spectroscopy combined with velocity map imaging techniques has also been employed to investigate the CD effect of gas-phase chiral molecules and clusters from single photon or multiphoton ionization¹⁸⁻²¹.

Recently, we developed a new CD technique for measuring the CD spectra of jet-cooled chiral molecules over a broad wavelength range²². In this technique, a photoelastic modulator (PEM) was used to generate alternating LCP and RCP pulses. This pulse-to-pulse alternation proved crucial in measuring the weak CD effects of jet-cooled molecules because it effectively reduces noises from short- and long-term variations in the laser-pulse energy and gas density. Using this CD technique, we obtained resonant two-photon ionization circular dichroism (R2PICD) spectra of pseudoephedrine (pED) and ephedrine (EPD) in a supersonic jet, which exhibited well-resolved CD bands that were specific to the conformations and vibrational modes.

R2PI is a two-photon process in which a molecule is excited by one-photon absorption and then ionized by a second photon. Thus, in principle, the R2PICD value represents the cumulative CD of both the excitation and ionization in the R2PI process, and it does not necessarily coincide with the conventional CD value from the one-photon absorption process. However, the CD effect of ionization can be very small because ionization involves transitions to a continuum of different states. The overlap of these different transitions in the ionization step may lead to leveling or canceling of the CD effects¹⁶. Therefore, the R2PICD value is predominantly determined by the CD of the excitation. This is further supported by the fact that the R2PICD values of a few organic compounds agree well with the CD measured in a conventional CD spectrometer¹⁴.

However, it is unfair to compare the R2PICD value of molecules in a supersonic jet with the CD value measured using a gas cell at room temperature. The molecules being compared should be under the same physical conditions. One method to accomplish this is to compare the R2PICD value with the fluorescence-detected circular dichroism (FD CD) of jet-cooled molecules, which measures the difference in the fluorescence yields of LCP and RCP pulses. Fluorescence excitation (FE) spectroscopy as a complementary technique to R2PI has

been extensively utilized to obtain electronic spectra of molecules in supersonic jets^{23,24}. It records the total laser-induced fluorescence (LIF) signals of molecules excited by one-photon absorption as a function of the laser wavelength. Thus, based on the generally valid assumption that the FE spectrum parallels the absorption spectrum²⁵, FDCD is considered to represent the CD of one-photon absorption, much like conventional CD.

Here, we obtained FDCD spectra of jet-cooled (1*S*,2*R*)-(+)- and (1*R*,2*S*)-(-)-ephedrine (+EPD and -EPD, respectively) for the first time using alternating LCP and RCP pulses generated with a PEM. The FDCD spectra exhibited well-resolved CD bands, which agreed well with the R2PICD spectra. However, certain CD bands in the FDCD spectra were opposite in sign to those in the R2PICD spectra. To understand why these CD signs were different, we measured the ultraviolet-ultraviolet (UV-UV) hole burning (HB) spectrum and the R2PI spectra recorded at different fragment mass channels. The vibrational modes were also assigned by comparing the experimental spectra with theoretical electronic spectra simulated using time-dependent density functional theory (TDDFT). We suggest that the different CD signs of the R2PICD and FDCD spectra may result from state-selective isomerization occurring at the intermediate state.

2 Methods

2.1 Experimental

The experimental set-up was described elsewhere²² and a brief description is given below. -EPD and (1*S*,2*R*)-(+)-ephedrine hydrochloride (+EPD•HCl) were purchased from Sigma-Aldrich. -EPD was used without further purification, and +EPD was prepared from +EPD•HCl following the procedure reported previously²⁶. Each of the powder samples was heated to 40 °C in the sample oven, and the vapor was co-expanded with helium at 3 bar through a pulsed nozzle. The expanding gas passed through a skimmer and entered the

ionization region of a time-of-flight (TOF) mass spectrometer. The EPD molecules in the ionization region were irradiated with an ultraviolet (UV) laser pulse for R2PI. The resulting ions were accelerated to the field-free region of the TOF mass spectrometer and detected by a microchannel plate.

For the FDCD spectra, the expanding gas through the pulsed nozzle was irradiated with a UV laser pulse at approximately 5 mm downstream from the nozzle hole. The LIF signal was collected with a biconvex lens and detected by a photomultiplier tube. The frequency-doubled output ($\sim 500 \mu\text{J}/\text{pulse}$, 10 ns) of the dye laser pumped by an Nd:YAG laser was used to obtain the R2PICD and FDCD spectra.

The conformation-specific FE spectrum was measured using UV-UV HB spectroscopy. The HB laser, which depletes the ground-state population of a specific conformer, was fixed to the wavenumber of a vibronic band, and the probe laser was scanned over the spectral range. The time delay between the HB and the probe laser was adjusted to 500 ns. The UV-UV HB spectrum was obtained by recording the difference between the fluorescence signals produced by the probe laser with and without irradiation of the HB laser. Linearly polarized laser pulses with an energy of $\sim 500 \mu\text{J}/\text{pulse}$ were used for the HB and the probe laser.

The LCP and RCP pulses were generated by passing UV laser pulses through a PEM (Hinds Instruments, Inc.) when its retardation values became $-\lambda/4$ and $+\lambda/4$, respectively. For this purpose, the oscillation of the retardation value and the laser firing was synchronized as follows. 50-kHz reference pulses from the PEM were down-counted to 10-Hz using a frequency divider. The 10-Hz pulse was then fed into two digital delay generators, DG1 and DG2, as a triggering pulse. DG1 and DG2 divided the 10-Hz pulses into two alternating 5-Hz pulses with time delays of δt_1 and δt_2 , respectively. The δt_1 and δt_2 values were adjusted such that the laser pulses fired by the 5-Hz pulses from DG1 and DG2 passed through the PEM

when its retardation became $-\lambda/4$ and $+\lambda/4$, respectively.

2.2 Theoretical

The geometries of the EPD conformers in the electronic ground and excited states were fully optimized at the M06-2X/6-311++G(d,p) level of theory²⁷. The vibrational frequencies were calculated at the same level to confirm that the optimized geometries were local minima in the potential energy surface. The rotatory strengths, R , were calculated using TDDFT at the M06-2X/6-311++G(d,p) level. The electronic spectra of EPD were simulated at the same level of theory with consideration of the Franck-Condon approximation. All calculations were performed using the Gaussian 09 (Revision D.01) software package²⁸.

3 Results and discussion

Figure 1a shows the R2PI spectrum of +EPD in a supersonic jet near the origin band of the S_0 - S_1 transition obtained by monitoring the fragment ion at a m/z (mass to charge ratio) of 58, which agrees well with previous results^{22,29}. Most of the peaks in the spectrum, including the A-C peaks, were assigned from the lowest-energy conformer AG(a)^{22,29}. The parent ions ($m/z=165$) are not detected in the mass spectrum because of efficient fragmentation following ionization³⁰. It was previously concluded that the fragmentation preferentially occurs in the EPD ion rather than in the neutral intermediate state, based on the followings²⁹⁻³¹. First, the two-photon excitation energy of one-color R2PI is much higher than the adiabatic ionization energy of EPD. Second, the fragment of $m/z=58$ is also a dominant fragment in the mass spectra obtained by electron impact ionization, chemical ionization, and fast atom bombardment³²⁻³⁴. Third, the similar ion fragmentation was observed in R2PI spectroscopy of amphetamine and phenylethylamine^{35,36}.

Figure 1b is the R2PICD spectra of +EPD and -EPD obtained by subtracting the ion

signals produced by the RCP pulses from those produced by the LCP pulses. Both spectra exhibited well-resolved CD bands, which were mirror images of each other. The CD sign of the B band was opposite to those of the A and C bands, which is consistent with the previous result²². The CD sign of origin band A agreed well with the sign of the rotatory strength R of AG(a) that was calculated using TDDFT at the M06-2X/6-311++G(d,p) level (Table 1S).

Figure 1c is the FE spectrum of +EPD, which shows the same spectral features as the R2PI spectrum. This indicates that the R2PI spectrum, although recorded at the fragment mass channel of $m/z=58$, represents the electronic spectrum of EPD. The peaks in the FE spectrum have slightly narrower bandwidths than those in the R2PI spectrum. The B band in the R2PI spectrum is resolved into two closely spaced bands at 526 and 530 cm^{-1} (B_1 & B_2 , respectively) from the origin band.

Figure 1d shows the FDCD spectra obtained by subtracting the total LIF signals produced by RCP pulses from those produced by LCP pulses. The FDCD spectra also exhibit well-resolved, mirror-image CD spectra. The CD signs of the A and C bands are consistent with those in the R2PICD spectra, but those of the B_1 and B_2 bands are opposite that of the B band.

The CD in ion or fluorescence yields is determined by the asymmetric factor g given by $g=2(I^L - I^R)/(I^L + I^R)$, where I^L and I^R are the ion or fluorescence signals produced by the LCP and RCP pulses, respectively^{12,37,38}. Table 1 lists the asymmetry factors, g_f and g_{r2pi} , of the A–C bands measured from the FDCD and R2PICD spectra, respectively. All g_f and g_{r2pi} values of the A–C bands are in the range of 1–2%. The g values for the ionization (g_i) following the excitation of the A–C bands are also estimated from g_f and g_{r2pi} values using the equation derived in the Supplementary Information. For the A band, the g_i value is nearly zero, implying little CD effect of the ionization, as suggested previously¹⁴. The CD effect of ionization is moderate for the C band, for which the g_i value is half of the g_f . The largest CD

effect of ionization is observed for the B band, for which the g_i value is two times larger than and has the opposite sign as g_f .

To understand the large CD effect of ionization of the B band, we first ensured that the A–C bands are from the same conformer, as suggested previously^{22,29}. Figures 2a and 2b show the FE and UV-UV HB spectra, respectively, and the latter is measured with the HB laser fixed at the A band. Nearly all bands in the FE spectrum, including the two bands at 526 and 530 cm^{-1} , appear as dip signals in the HB spectrum. This result confirms that the A–C bands are indeed from a single conformer.

Second, we measured the number of photons involved in the R2PI process to determine whether more than two photons are absorbed to generate the ion signals of the B band. The ion intensities (I_{ion}) as a function of the laser intensity (P) were measured with the laser fixed at the A and B bands. The slopes in the plots of $\log I_{\text{ion}}$ versus $\log P$ were all fit to 1.8, thus indicating that only two-photons were involved in generating the ion signals (Fig. 1S). Thus, we confirmed that the g_i values in Table 1 represent the CD of one-photon ionization following excitation of the A–C bands.

Third, we obtained the R2PI spectra recorded at two different fragment mass channels, $m/z=71$ and 85 (Fig. 3). The ion signals at these mass channels are an order of magnitude less than those at $m/z=58$. Interestingly, the fragment ions of $m/z=71$ and 85 are largely produced by excitation of the B band, not the A or C bands. The bands at -4 and -11 cm^{-1} in Figures 3b and c, respectively, were assigned previously as hot bands²⁹. The fragment ions of $m/z=71$ and 85 are generated by excitations of the bands at 526 and 530 cm^{-1} and at 519 and 526 cm^{-1} , respectively. The band at 519 cm^{-1} is not observed in the R2PI spectrum recorded at $m/z=58$. These results imply that the excitation of the B band opens new fragmentation pathways that are not accessible by excitation of the A or C bands.

Neusser and coworkers²⁹ suggested possible fragmentation pathways yielding the fragments of $m/z=71$ and 85. For the fragment of $m/z=71$, two possible pathways originated from the most stable conformers, AG(a) and GG(a), were proposed. For the fragment of $m/z=85$, one single pathway from the GG(a) was suggested. All of the bands at 519, 526, and 530 cm^{-1} were previously assigned to the AG(a). Thus, to explain the state-selective fragmentation yielding the fragments of $m/z=71$ and 85 from the GG(a), it was insisted that the isomerization from AG(a) to GG(a) occurs after excitation of those bands.

The anomalously large CD effect of ionization of the B band may also be explained by the state-selective isomerization. A large structural change resulting from this isomerization may lead to sign inversion of the CD of ionization from the CD of excitation. Previous research determined that the CD sign of 3-MCP measured by REMPI was inverted when fragmented into a daughter ion following isomerization of the molecular ion³⁹.

To understand why the excitation of only the B band, not the A or C bands, leads to isomerization, we assigned the vibrational modes of these bands by comparing the FE spectrum with the theoretical one simulated using TDDFT with consideration of the Franck-Condon factors (Fig. 2S). Based on the agreement between the experimental and theoretical spectra, the B_1 and B_2 bands were identified as out-of-plane ring bending and in-plane ring deformation modes, respectively, and the C band corresponded to a symmetric ring stretching mode (Fig. 4).

These assignments support the state-selectivity of the B band in the isomerization process. For the isomerization from AG(a) to GG(a) to occur, the side groups attached to the C2 atom need to rotate by $\sim 120^\circ$ around the C1-C2 bond (Fig. 4). This rotation seems to be facilitated by the vibrational modes of the B_1 and B_2 bands, in which torsional motions of the C2-H bond around the axis of the C1-C2 bond (red arrows in Fig. 4) are activated along with the asymmetric ring distortion. In contrast, no such torsional motions are induced in the

vibrational mode of the C band. Further investigation using picosecond pump-probe time-resolved spectroscopy may be necessary not only to confirm the occurrence of the isomerization but also to provide further insight into the state-selective process.

4 Conclusions

FDCD spectra of jet-cooled EPD were obtained to measure the CD of one-photon absorption and thus to investigate the CD effect of ionization in R2PI by comparison with the R2PICD spectra. The CD effects of ionization following the excitation of the A and C bands were very small, whereas that of the B band was anomalously large, leading to inversion of the CD sign between the FDCD and R2PICD spectra. Based on the state-selective fragmentation patterns in R2PI, we suggested that this large CD effect is due to the state-selective isomerization that occurs after excitation of the B band. The state selectivity of the isomerization was further supported by the vibrational mode of the B band, which facilitates isomerization by activating the torsional motions of the side chain. This study demonstrates that FDCD spectroscopy of jet-cooled chiral molecules is an effective method to measure the CD value of one-photon absorption, which can be directly compared with theoretical and conventional CD values, thus facilitating the development of theory to predict accurate CD values. Furthermore, combined with R2PICD spectroscopy, FDCD spectroscopy can provide a powerful tool to investigate the CD effects of excitation and ionization processes separately in R2PI and thus probe any structural variations that occur during the ionization process.

5 Acknowledgment

This work was supported by the research grant of the Chungbuk National University in 2013, the Korea Basic Science Institute Grant (D35613), and the Basic Science Research Program through the National Research Foundation of Korea (NRF) funded by the Ministry

of Education, Science and Technology (NRF-2013R1A2A2A01014547 (NJK) and 2014R1A1A2055150 (JH)). We thank Prof. Hyo Won Lee for providing the purified sample.

Electronic supplementary information (ESI) available. See DOI:

References

- 1 A. Cotton, *C. R. H. Acad. Sci.*, 1895, **120**, 989-991.
- 2 N. Berova, L. D. Bari and G. Pescitelli, *Chem. Soc. Rev.*, 2007, **36**, 914-931.
- 3 I. Warnke and F. Furche, *WIREs Comput. Mol. Sci.*, 2012, **2**, 150-166.
- 4 S. Ionescu, I. Matei, C. Tablet and M. Hillebrand, *Phys. Chem. Chem. Phys.*, 2013, **15**, 11604-11614.
- 5 N. Kobayashi, A. Muranaka and J. Mack, *Circular dichroism and magnetic circular dichroism spectroscopy for organic chemists*, The Royal Society of Chemistry, Cambridge, 2012.
- 6 G. Pescitelli, V. Barone, L. D. Bari, A. Rizzo and F. Santoro, *J. Org. Chem.*, 2013, **78**, 7398-7405.
- 7 A. Zehnacker and M. A. Suhm, *Angew. Chem. Int. Ed.*, 2008, **47**, 6970-6992.
- 8 F. Pulm, J. Schramm, J. Hormes, S. Grimme and S. D. Peyerimhoff, *Chem. Phys.*, 1997, **224**, 143-155.
- 9 M. G. Mason and O. Schnepp, *J. Chem. Phys.*, 1973, **59**, 1092-1098.
- 10 K. P. Gross and O. Schnepp, *J. Chem. Phys.*, 1978, **68**, 2647-2657.
- 11 P. Brint, E. Meshulam and A. Gedanken, *Chem. Phys. Lett.*, 1984, **109**, 383-387.
- 12 R. Li, R. Sullivan, W. Al-Basheer, R. M. Pagni and R. N. Compton, *J. Chem. Phys.*, 2006, **125**, 144304.
- 13 H. G. Breunig, G. Urbasch, P. Horsch, J. Cordes, U. Koert and K.-M. Weitzel, *ChemPhysChem*, 2009, **10**, 1199-1202.
- 14 C. Loge and U. Boesl, *ChemPhysChem*, 2011, **12**, 1940-1947.
- 15 C. Loge, A. Bornschlegl and U. Boesl, *Int. J. Mass Spectrom.*, 2009, **281**, 134-139.
- 16 U. Boesl, A. Bornschlegl, C. Loge and K. Titze, *Anal. Bioanal. Chem.*, 2013, **405**, 6913-6924.
- 17 K. Titze, T. Zollitsch, U. Heiz and U. Boesl, *ChemPhysChem*, 2014, **15**, 2762-2767.

- 18 I. Powis, S. Daly, M. Tia, B. C. de Miranda, G. A. Garcia and L. Nahon, *Phys. Chem. Chem. Phys.*, 2014, **16**, 467-476.
- 19 C. Lux, M. Wollenhaupt, T. Bolze, Q. Liang, J. Kohler, C. Sarpe and T. Baumert, *Angew. Chem. Int. Ed.*, 2012, **51**, 5001-5005.
- 20 M. H. M. Janssen and I. Powis, *Phys. Chem. Chem. Phys.*, 2014, **16**, 856-871.
- 21 S. Turchini, D. Catone, N. Zema, G. Contini, T. Prospero, P. Decleva, M. Stener, F. Rondino, S. Piccirillo, K. C. Prince and M. Speranza, *ChemPhysChem*, 2013, **14**, 1723-1732.
- 22 A. Hong, C. M. Choi, H. J. Eun, C. Jeong, J. Heo and N. J. Kim, *Angew. Chem. Int. Ed.*, 2014, **53**, 7805-7808.
- 23 R. E. Smalley, D. H. Levy and L. Wharton, *J. Chem. Phys.*, 1976, **64**, 3266-3276.
- 24 M. S. de Vries and P. Hobza, *Ann. Rev. Phys. Chem.*, 2007, **58**, 585-612.
- 25 D. H. Turner, I. Tinoco Jr. and M. Maestre, *J. Am. Chem. Soc.*, 1974, **96**, 4340-4342.
- 26 T. Q. Chou, *J. Biol. Chem.*, 1926, **70**, 109-114.
- 27 J. L. Alonso, M. E. Sanz, J. C. Lopez and V. Cortijo, *J. Am. Chem. Soc.*, 2009, **131**, 4320-4326.
- 28 Gaussian 09, Revision **D.01**, M. J. Frisch, G. W. Trucks, H. B. Schlegel, G. E. Scuseria, M. A. Robb, J. R. Cheeseman, G. Scalmani, V. Barone, B. Mennucci, G. A. Petersson, H. Nakatsuji, M. Caricato, X. Li, H. P. Hratchian, A. F. Izmaylov, J. Bloino, G. Zheng, J. L. Sonnenberg, M. Hada, M. Ehara, K. Toyota, R. Fukuda, J. Hasegawa, M. Ishida, T. Nakajima, Y. Honda, O. Kitao, H. Nakai, T. Vreven, J. A. Montgomery, Jr., J. E. Peralta, F. Ogliaro, M. Bearpark, J. J. Heyd, E. Brothers, K. N. Kudin, V. N. Staroverov, R. Kobayashi, J. Normand, K. Raghavachari, A. Rendell, J. C. Burant, S. S. Iyengar, J. Tomasi, M. Cossi, N. Rega, J. M. Millam, M. Klene, J. E. Knox, J. B. Cross, V. Bakken, C. Adamo, J. Jaramillo, R. Gomperts, R. E. Stratmann,

- O. Yazyev, A. J. Austin, R. Cammi, C. Pomelli, J. W. Ochterski, R. L. Martin, K. Morokuma, V. G. Zakrzewski, G. A. Voth, P. Salvador, J. J. Dannenberg, S. Dapprich, A. D. Daniels, Ö. Farkas, J. B. Foresman, J. V. Ortiz, J. Cioslowski, and D. J. Fox, Gaussian, Inc., Wallingford CT, 2009.
- 29 R. Karaminkov, S. Chervenkov, P. Harter and H. J. Neusser, *Chem. Phys. Lett.*, 2007, **442**, 238-244.
- 30 P. Butz, R. T. Kroemer, N. A. Macleod and J. P. Simons, *J. Phys. Chem. A*, 2001, **105**, 544-551.
- 31 S. Chervenkov, P. Q. Wang, J. E. Braun and H. J. Neusser, *J. Chem. Phys.*, 2004, **121**, 7169-7174.
- 32 T. L. Barry and G. Petzinger, *Biol. Mass Spectrom.*, 1977, **4**, 129-133.
- 33 Y. Marde and R. Ryhage, *Clin. Chem.*, 1978, **24**, 1720-1723.
- 34 F. Brazzarola, M. Tubaro, P. Bravo, M. Zanda, A. Volonterio and P. Traldi, *Il Farmaco*, 2003, **58**, 69-77.
- 35 J. Yao, H. S. Im, M. Foltin and E. R. Bernstein, *J. Phys. Chem. A*, 2000, **104**, 6197-6211.
- 36 J. A. Dickinson, M. R. Hockridge, R. T. Kroemer, E. G. Robertson, J. P. Simons, J. McCombie and M. Walker, *J. Am. Chem. Soc.*, 1998, **120**, 2622-2632.
- 37 A. Bornschlegl, C. Loge and U. Boesl, *Chem. Phys. Lett.*, 2007, **447**, 187-191.
- 38 P. Horsch, G. Urbasch, K.-M. Weitzel and D. Kroner, *Phys. Chem. Chem. Phys.*, 2011, **13**, 2378-2386.
- 39 C. Loge and U. Boesl, *Phys. Chem. Chem. Phys.*, 2012, **14**, 11981-11989.

Figure captions

Figure 1. (a) R2PI spectrum of +EPD recorded at the fragment mass channel of $m/z=58$. (b) R2PICD spectra of +EPD (blue) and -EPD (red) obtained by subtracting the ion signals produced by RCP pulses from those by LCP. (c) FE spectrum of +EPD, which is exactly the same with that of -EPD. The numbers represent the relative wavenumbers of the bands with respect to the origin band A. (d) FDCD spectra of +EPD (blue) and -EPD (red) obtained by subtracting the total fluorescence signals produced by RCP pulses from those by LCP.

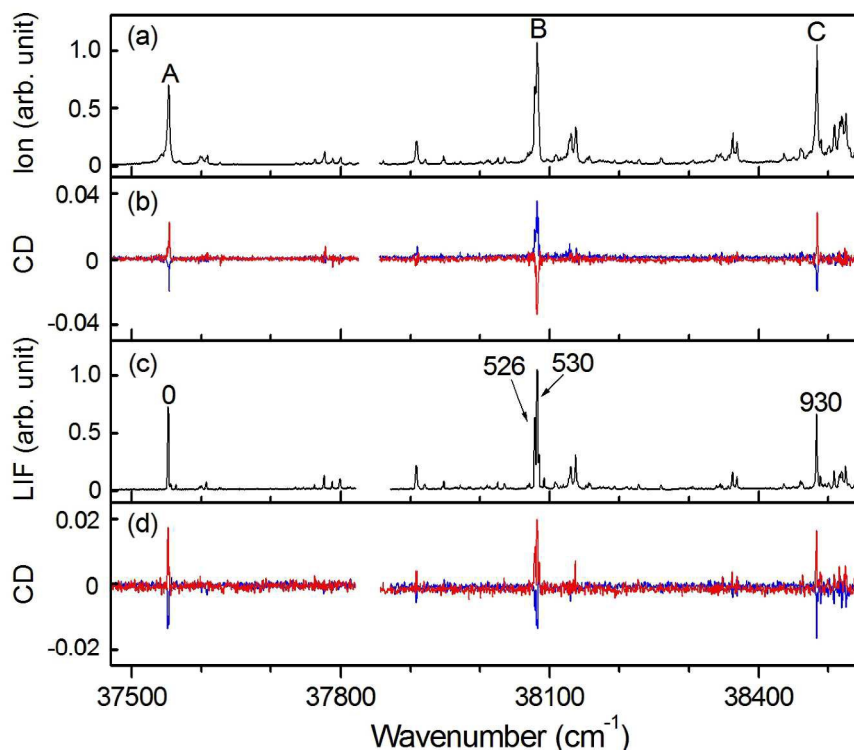
Figure 2. (a) FE and (b) UV-UV HB spectra of +EPD. The UV-UV HB spectrum is measured with the HB laser fixed at the origin band A. The inset is an enlarged view of the B band, which is resolved into two bands at 526 and 530 cm^{-1} from the origin band.

Figure 3. R2PI spectra recorded at the fragment mass channels of (a) $m/z=58$, (b) 71, and (c) 85. The numbers indicate the relative wavenumbers of each band from the origin band. The bands at -4 and -11 cm^{-1} were previously assigned as hot bands. The inset shows the structures of the corresponding fragment ions.

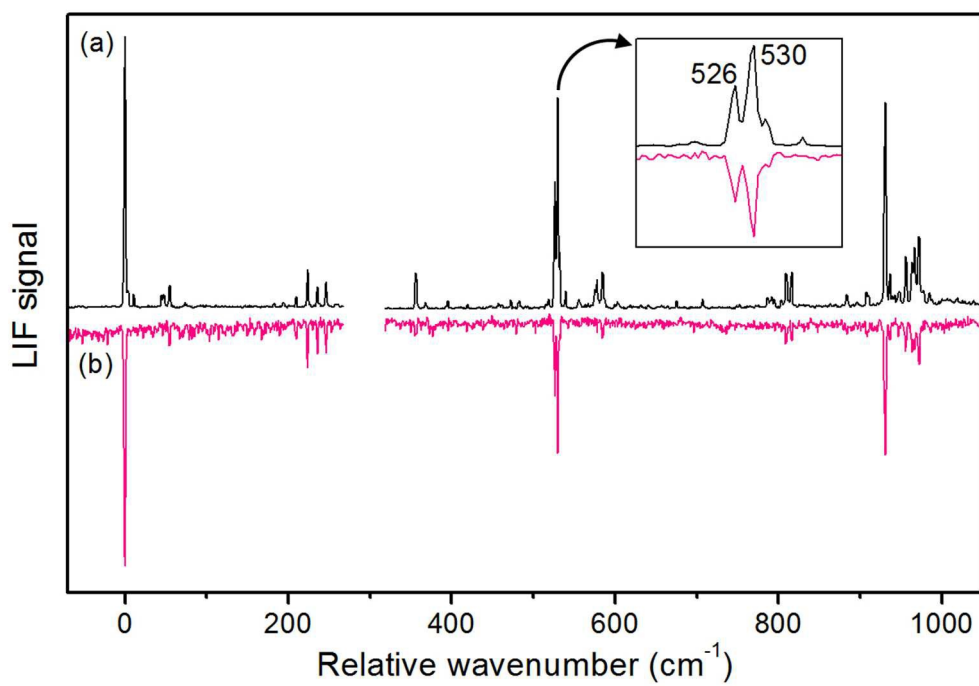
Figure 4. Pictorial representations of the vibrational modes of the (a) B_1 , (b) B_2 , and (c) C bands. The arrows represent the displacements of atoms during the vibrational motion. The red arrows indicate torsional motions of the side chain, which may facilitate the isomerization process.

Table 1. Asymmetric factors g of the A-C bands.

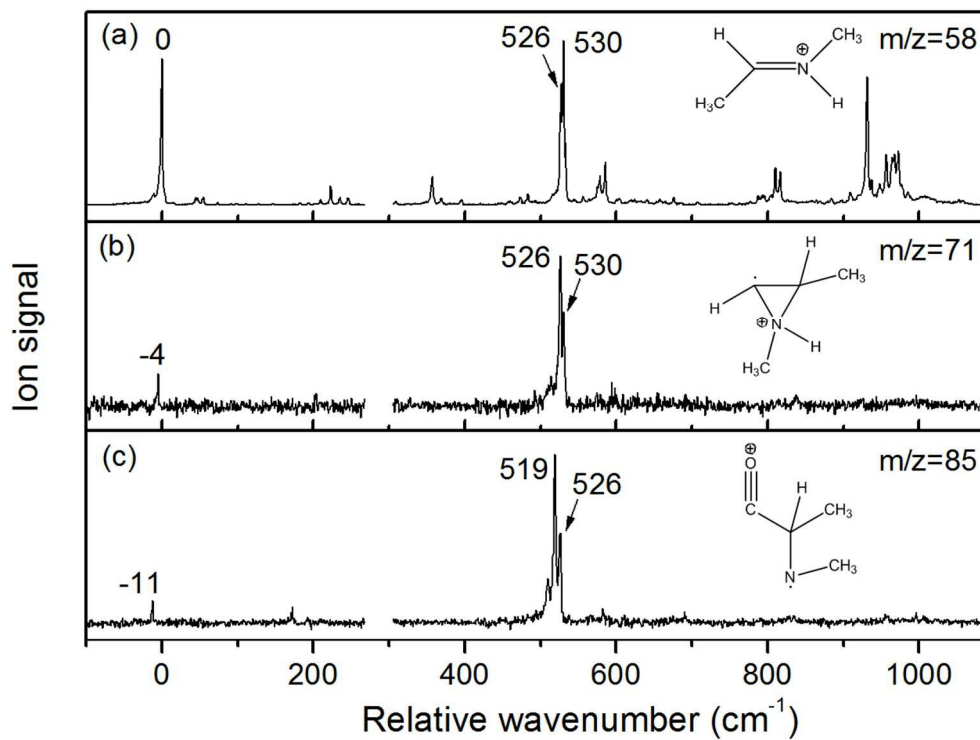
$g(\%)$		A	B		C
			B_1	B_2	
g_f	+EPD	-2.0 ± 0.7	-1.5 ± 0.2	-1.5 ± 0.1	-1.5 ± 0.1
	-EPD	1.7 ± 0.4	1.4 ± 0.1	1.4 ± 0.1	1.3 ± 0.1
g_{r2pi}	+EPD	-1.9 ± 0.1		2.0 ± 0.5	-2.4 ± 0.2
	-EPD	1.8 ± 0.5		-1.9 ± 0.2	2.0 ± 0.1
g_i	+EPD	0.1 ± 0.8		3.5 ± 0.6	-0.9 ± 0.3
	-EPD	0.1 ± 0.9		-3.3 ± 0.3	0.7 ± 0.2



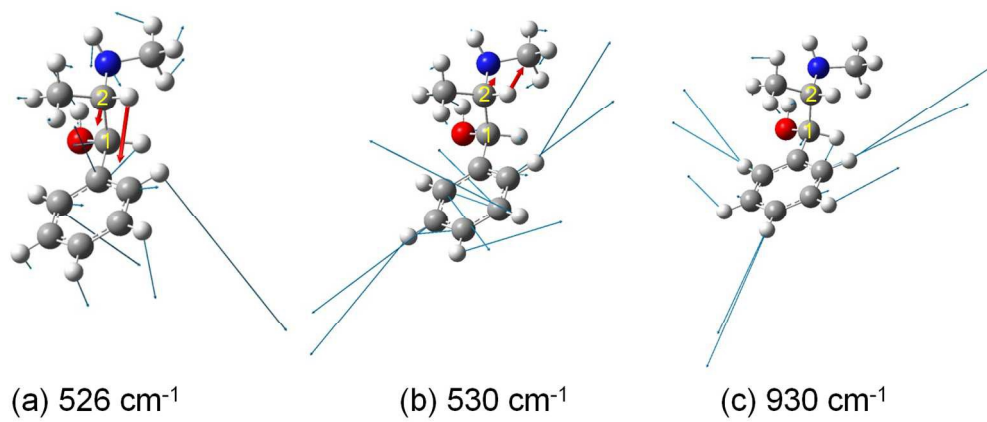
279x215mm (300 x 300 DPI)



435x307mm (72 x 72 DPI)



451x337mm (72 x 72 DPI)



603x258mm (72 x 72 DPI)